Stable confinement of toroidal electron plasma in an internal conductor device Prototype-Ring Trap

H. Saitoh,[a] Z. Yoshida, and S. Watanabe
Graduate School of Frontier Sciences, University of Tokyo, 5-1-5 Kashiwanoha, Kashiwa, Chiba 277-8583, Japan

(Received 29 November 2004; accepted 8 July 2005; published online 26 August 2005)

A pure electron plasma has been produced in an internal conductor device Prototype-Ring Trap (Proto-RT). The temporal evolution of the electron plasma was investigated by the measurement of electrostatic fluctuations. Stable confinement was realized when the potential profile adjusted to match the magnetic surfaces. The confinement time varies as a function of the magnetic field strength and the neutral gas pressure, and is comparable to the diffusion time of electrons determined by the classical collisions with neutral gas. Although the addition of a toroidal magnetic field stabilized the electrostatic fluctuation of the plasma, the effects of the magnetic shear shortened the stable confinement time, possibly because of the obstacles of coil support structures. © *2005 American Institute of Physics*. [DOI: 10.1063/1.2011405]

I. INTRODUCTION

Several studies have focused on the confinement of non-neutral plasmas in toroidal geometries.[1–6] The early experiments aimed at the storage or acceleration of heavy ions[2] or creation of high-current relativistic electron beams[3] in a pure toroidal magnetic field configuration. In recent years, it has been recognized that the toroidal geometries might be suitable for various kinds of non-neutral plasmas,[7,8] such as the mixtures of antimatters[9] or streaming non-neutralized plasmas for the investigation of new relaxation states of plasmas with strong flow.[7] At present, experiments of toroidal non-neutral plasmas on internal conductor devices,[7] a "partial" torus trap,[10,11] a stellarator,[9] and a helical system[12] are in progress or under construction.

For the confinement of non-neutral plasmas in open field linear devices, which are most generally used, charged particles are confined by the combination of a homogeneous magnetic field and an electrostatic potential well.[13] In the Malmberg–Penning traps, Lorentz force due to the rigid rotating $\mathbf{E}\times\mathbf{B}$ motion balances the repulsive self-electric field of the non-neutral plasma and centrifugal force, where the flow has no shear and the plasma may come to a thermal equilibrium state. Due to the many experimental techniques, including the use of multi-ring electrodes for the reduction of image charge effects,[14] compensation of the slowly damping torque of the plasma by a "rotating wall" external electric field,[15] together with the use of ultra-high vacuum and precisely aligned symmetric field and device geometry, extremely long confinement of non-neutral plasmas has been realized in linear devices. In contrast to the linear devices, toroidal configurations use no electric fields along the magnetic field lines, and thus have an ability to confine charged particles at any degree of non-neutrality. Although several theoretical works including those on equilibrium[9] and stability[16] have been carried out, little is known about the experimental issues of the confinement properties of non-neutral plasmas in the magnetic surface configuration. Magnetic surfaces are defined as $\psi(\mathbf{r})=\text{const}$ planes, where magnetic field lines lie on, and thus $\nabla\psi(\mathbf{r})\cdot\mathbf{B}=0$ is satisfied. In a toroidally symmetric configuration $(\partial/\partial\theta=0)$, magnetic surfaces are given by $\psi(r,z)=rA_\theta$, where $A_\theta(r,z)$ is the azimuthal component of the vector potential $\mathbf{A}$. When the canonical angular momentum of a particle is conserved

$$P_\theta=\frac{\partial L}{\partial\dot{\theta}}=mr^2\dot{\theta}+qrA_\theta=\text{const},$$

the spatial deviation d of a particle from a magnetic surface is comparable to or smaller than the poloidal Larmor radius r_p:

$$d\lesssim r_p\equiv\left|\frac{mr\dot{\theta}}{qB_p}\right|,$$

where m is the mass, $r\cdot\theta$ is the velocity, q is the charge of the particle, and $B_p=\sqrt{B_r^2+B_z^2}$ is the poloidal magnetic field strength. When the magnetic field is strong and the mechanical momentum of the particle is ignored, the particle motion is limited on a magnetic surface. This is the basic mechanism for the confinement of charged particles in a magnetic surface configuration, which also applies to usual neutral plasmas.

The present study describes the confinement properties of a toroidal pure electron plasma in a magnetic surface configuration in the Proto-RT (Prototype-Ring Trap) device. When an external electric field is applied[6,10,11,17] and the potential profile is modified by a ring electrode to adjust to the magnetic contours of the applied dipole magnetic field, the oscillation of the diocotron mode is stabilized and the plasma enters a stable oscillation mode. The obtained confinement time is in the order of 0.1 s, which is close to the time scale of the diffusion of electrons due to the collisions with neutral gas. The stable confinement time is determined by the strength of the magnetic field and the background neutral gas pressure, indicating that collisional processes with neutral

[a]Electronic mail: saito@ppl.k.u-tokyo.ac.jp

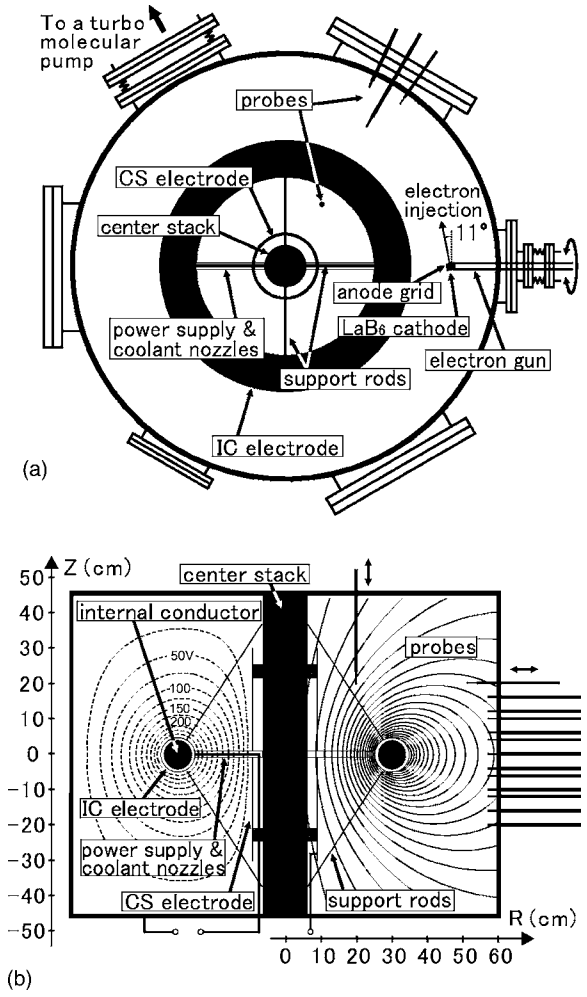

FIG. 1. Schematic of Proto-RT chamber. (a) Top view and (b) poloidal cross-section, magnetic surfaces of dipole field (solid lines), and vacuum electrostatic potential contours (dotted lines) when IC electrode is biased to $V_{IC}=+300$ V and CS electrode is shorted to the chamber.

atoms set the upper limit of the confinement time. The effects of magnetic shear on the toroidal electron plasma were also tested by adding a toroidal field to the dipole field configuration. The propagating direction and the amplitude of the electrostatic fluctuations of the plasma were measured by wall probes located in the same poloidal cross section of the device. The device setup, diagnostics by electrostatic probes, and experimental results are described in the following sections.

II. EXPERIMENTAL SETUP AND FORMATION OF ELECTRON PLASMA

A. Toroidal confinement device and measurements

The experiment was carried out at Proto-RT, a toroidal internal ring device. The objectives of the Proto-RT project and a detailed description of the machine parameters are summarized in Ref. 7. Figure 1 shows the schematic view of the Proto-RT. The chamber has an inner radius of 59 cm and a height of 90 cm, and is evacuated to a base pressure of 4×10^{-7} Torr by a turbomolecular pump. Magnetic fields are generated by an internal conductor (IC), vertical field (VF) coils, and toroidal field (TF) coils. The IC is suspended by stainless (SUS 304) support rods that are covered with insulating ceramic tubes. The major radius of the IC is 30 cm. A pair of VF coils and TF coils are located outside the chamber. The coil currents supplied by dc power sources are IC: 10.5 kAT, VF: 5.25 kAT, and TF: 30 kAT, respectively. The bar structures for the IC power feed and coil cooling are also covered by ceramic tubes for insulation.

A torus-shaped electrode covers the surface of the IC, and its minor radius and surface area are 5 cm and 0.59 m^2, respectively. A bias voltage, V_{IC}, of −400 V to +400 V is applied to the IC electrode against the vessel wall by a dc power source. Another electrode is also installed on a center stack (CS), and in this experiment, was electrically shorted to the chamber ($V_{CS}=0$ V). In order to minimize the distortion of the electric fields, the feeder cables were covered by grounded stainless tubes and located along the CS. The vacuum equipotential surfaces generated by the electrodes are shown in Fig. 1.

The electrostatic potential of the electron plasma was measured by emissive Langmuir probes. It provided information on potential profiles during the electron injection phase with fine spatial resolution. The probes were arranged as an array and two-dimensional potential structures were measured in the confinement region. The probe tip is a thoria-tungsten spiral filament of 0.1 mm diameter heated by a dc current and operated in the space charge limited region. It was terminated to the chamber across high impedance (100 MΩ) voltage probes and used as floating probes.

After the electron supply was stopped, Langmuir probes placed inside the confinement region presented serious obstacles for the realization of stable equilibrium. For the measurement of electrostatic fluctuations and determination of the confinement time of the plasma without such perturbations, 5×15 mm and 5×250 mm copper foils were covered by insulating quartz tubes, installed in the chamber, and used as wall probes.[2,10] The sensor foil was connected to the vessel wall through a current amplifier for the observation of the image current, which indicates the motion of the plasma. The longer wall was placed over the entire confinement region and used for the estimation of the remaining charge of the plasma by integrating the passing image current.

B. Formation of electron plasma

Electrons were injected by an electron gun located at $R=46.5$ cm. An acceleration voltage of up to $V_{acc}=1.2$ kV can be applied between a LaB_6 cathode and a molybdenum anode grid of 65% transparency, located 2 mm in front of the cathode. The obtained maximum drain current is ~0.8 A ($V_{acc}=1.2$ kV, no magnetic field). The injection angle of the electron gun was decided according to a numerical calculation[18] so that the electrons take sufficiently long orbits. Examples of the orbits of a single electron in the typical dipole magnetic field configuration of Proto-RT are shown in Fig. 2. Some of the electrons were mirror reflected because of the inhomogeneous field strength of the dipole field, and trapped in the weaker field region. A detailed numerical investigation of the electron orbit in Proto-RT is described in

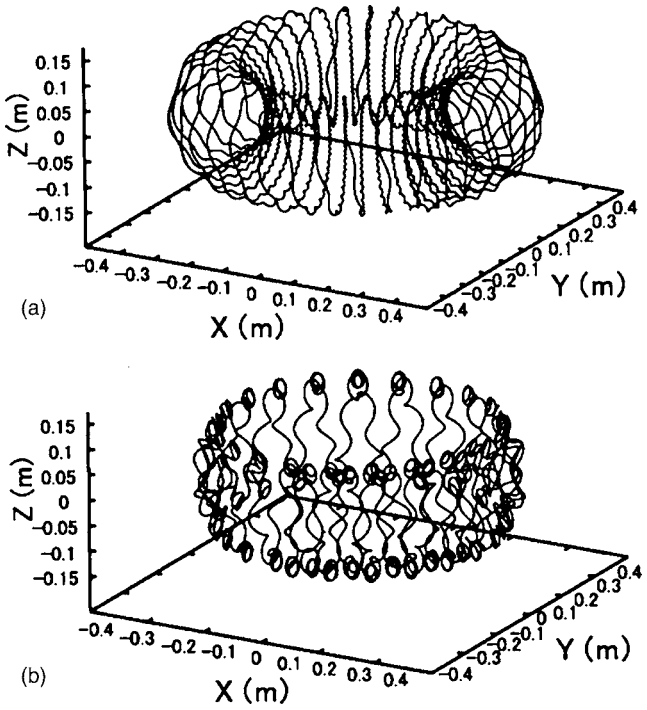

FIG. 2. The typical single electron orbits in a vacuum dipole magnetic field of Proto-RT (a) rotating around the internal conductor and (b) trapped due to magnetic mirror. The center axis of the device is X=Y=0. The electrons are injected from the midplane of the device at R=46.5 cm with the accelerating voltage of the electron gun of V_{acc}=300 V. The dipole field is generated by the internal conductor current of I_{IC}=7 kAT.

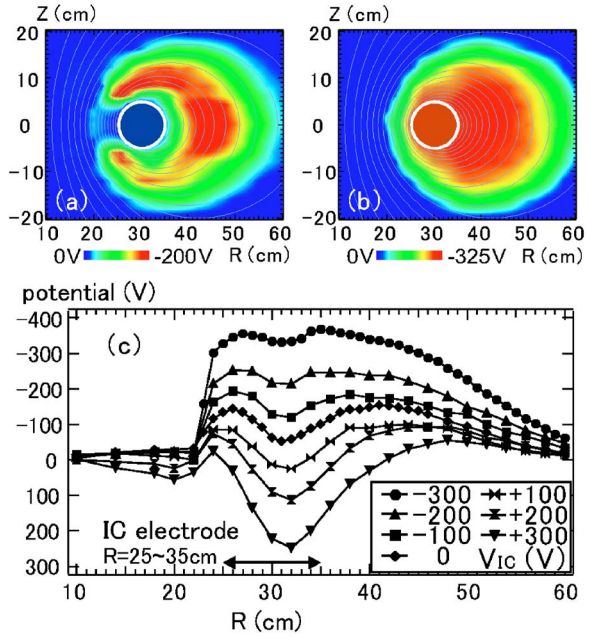

FIG. 3. (Color online). Two-dimensional potential profiles when (a) V_{IC} =0 V and (b) V_{IC}=−300 V. (c) Radial potential profiles at Z=+6 cm in the variation of the potential of the IC electrode, V_{IC}. Electrons are injected by an acceleration voltage of V_{acc}=300 V.

Refs. 18 and 19. In the toroidal direction, the electrons were transported due to the $\mathbf{E}\times\mathbf{B}$, ∇B, and curvature drifts. Electrons are injected for the period of typically ~100 μs, and the observed space potentials kept almost constant values during the injection phase. Although Langmuir probe characteristics show that the plasma has a thermalized bulk component, we observed no ion current in the current-voltage curves. The detection limit of the ion density by the present Langmuir probe is $\sim 10^{13}$ m^{-3}, assuming that the unmeasured ion temperature is 0.1 eV. It is possible that the thermalization process of the electrons is caused by collisions with remaining neutrals, and a small amount of low temperature ions exists in the plasma below the detection limit. The electrostatic potential profiles of the electron plasma were measured in several poloidal cross sections of Proto-RT,[18,19] and it was observed that the space potential is approximately a function of magnetic flux ψ in a pure dipole field configuration.

The potential profiles during the electron injection phase are shown in Fig. 3. When the potential is not externally controlled (the IC electrode is grounded) in Fig. 3(a), the distribution has a reversed "C" shape and the potential contours show strong disagreement with the magnetic surfaces of the dipole field configuration. When the temperature and neutral collisional effects are neglected in the force balance equation of the equilibrium state of the electron plasma, the perpendicular velocity of the electron is given by the $\mathbf{E}\times\mathbf{B}$ drift motion, and the electrostatic potential ϕ must be constant on a magnetic surface in the equilibrium states:[9] $\mathbf{B}\cdot\nabla\phi=0$. If this is the case during the electron injection in the present experiment, where the electron number density is far below the Brillouin density limit of $n_B \sim 10^{14}$ m^{-3} and the electron temperature is relatively low [measurement by Langmuir probes shows that the temperature of the bulk electrons is less than $T_e \sim 50$ eV (Ref. 18)], the disagreement of the contours of ϕ and ψ when $V_{IC} \geqslant 0$ implies that thermalized (low energy) electrons are not confined when the potential is not externally controlled.

In contrast, when the IC electrode is negatively biased comparable to the voltage of V_{acc} in Fig. 3(b), the potential hall near the IC electrode is eliminated, and the potential contours surround the IC, which is topologically close to the shape of the magnetic surfaces. By negatively biasing the IC electrode, the hollow structures are canceled, as illustrated in the radial potential profiles at Z=+6 cm (just above the IC electrode) in Fig. 3(c), which might lead to stabilizing the diocotron (Kelvin–Helmholtz) instability of non-neutral plasmas. As described in the next subsection, the measurements of electrostatic fluctuation show that the confinement time is enhanced for more than an order of magnitude by the negative bias of the IC.

By solving the Poisson equation,[20] we may reproduce the measured potential profile, assuming an electron cloud with a peak number density of 1×10^{13} m^{-3} and a total space charge of 3×10^{-7} C for V_{IC}=0 V. The high density region is relatively far from the support rods of the internal conductor throughout the experiments, and these structures do not seriously perturb the electron plasmas so long as the electrons rotate in the toroidal direction. When V_{IC}=−300 V, the peak density and total charge are estimated to be 1×10^{13} m^{-3} and 4×10^{-7} C, respectively.

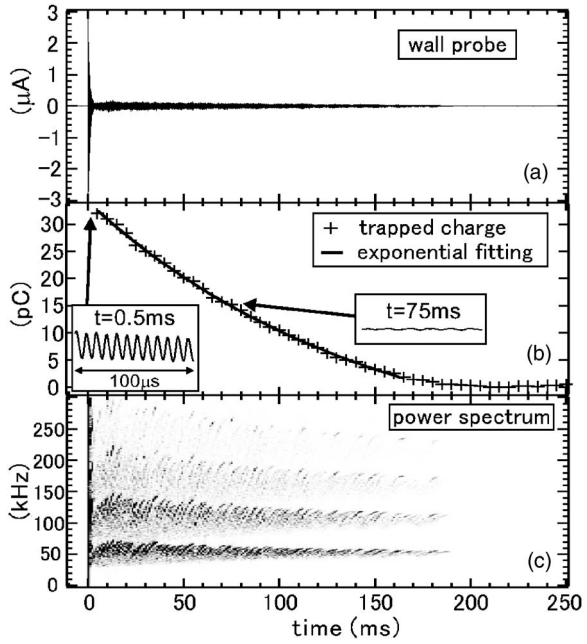

FIG. 4. (a) The typical waveform of a wall probe signal, (b) remaining charge on a wall and horizontal enlargement (for 100 μs) of the fluctuations of the remaining charge (small boxes, same vertical scale), and (c) power spectrum of the wall signal when the IC electrode is biased to −300 V. The electron gun was operated from $t=-100$ to 0 μs.

III. EXPERIMENTAL RESULTS

A. Confinement time and trapped charge

The temporal evolution of the electron plasma was investigated by measuring the electrostatic fluctuations. Figure 4 shows the typical waveform of the wall probe when $V_{IC}<0$ V, together with the trapped charge on the wall and power spectrum of the fluctuation. Electrons were injected with an acceleration voltage of 300 V from $t=-100$ to 0 μs into the dc magnetic and electric fields generated by a dipole field coil current of $I_{IC}=7$ kAT (magnetic field strength at $R=40$ cm is 70 G) and electrode bias voltages of $V_{IC}=-300$ V and $V_{CS}=0$ V. After the electron gun was turned off at $t=0$ s, a large oscillation during the electron injection phase decayed typically in a time constant of ~1 ms. Subsequently, a quiet oscillation mode was realized only when the IC electrode was negatively biased. The wall signals before and after the stabilization of the initial large fluctuation are shown in the small boxes in Fig. 4(b). The magnitude of the electrostatic fluctuation before and during the quiet mode normalized by the dc electrostatic potential in the plasma was $\tilde{\phi}/\phi=12\%$ and 0.6%, respectively. In the quiet confinement phase, the remaining charge drops approximately exponentially, as indicated in Fig. 4(b). As the plasma enters the quite confinement mode, the frequency of oscillation, illustrated in Fig. 4, decreased from 240 kHz to 62 kHz. In the quiet confinement phase, the decrease of the frequency was relatively small, and the peak of the fundamental frequencies in the power spectrum were 62 kHz at $t=5$ ms and 57 kHz at $t=180$ ms, indicating that both self- and external electric fields decide the frequencies of the electrostatic oscillation.

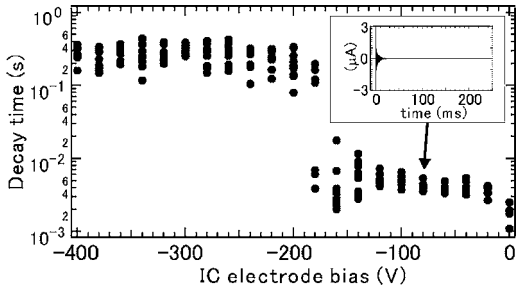

FIG. 5. Confinement time as a function of the bias voltage of the IC electrode, V_{IC}, and waveform of the wall when $V_{IC}=-80$ V.

The confinement time of the particles (time constants of the exponential fitting curves) as a function of V_{IC} is shown in Fig. 5. When V_{IC} is above −180 V, the initial fluctuation of the plasma does not enter a quiet state, and the charge decays within some milliseconds. As shown in the small box in Fig. 5, the amplitude of the initial fluctuation when $V_{IC}=-80$ V is $\tilde{\phi}/\phi=32\%$ and it decays without entering the quiet confinement mode. As indicated in Fig. 3(c), a drastic improvement of the confinement is observed when the hollow potential structure is eliminated by the sufficient bias voltage of the IC electrode.

Figure 6 shows the confinement time τ of electrons as a function of the background neutral gas (hydrogen) pressure P. At the base pressure of 4×10^{-7} Torr and the maximum dipole field coil current of 10.5 kAT, the obtained confinement time is $\tau=0.5$ s. When the confinement time of electrons is determined by the loss of the momentum of toroidal $\mathbf{E}\times\mathbf{B}$ motion due to the collisions with neutral gas, the toroidal viscous force is balanced by the Lorentz force caused by the outgoing radial velocity of electrons (neglecting the small inertia term):

$$0=-en_e v_r B-m_e n_e \nu_{en}(v_t-v_n),$$

where e is the charge, v_r and v_t are the radial and toroidal speed of electrons, m_e is the electron mass, n_e is the electron density, v_n is the velocity of the neutral atom, $\nu_{en}=n_n\sigma v_t$ is the electron-neutral atom mean collision frequency, n_n is the neutral gas density, and σ is the collision cross section. Assuming that $v_n=0$, the typical diffusion time of the electrons is given by

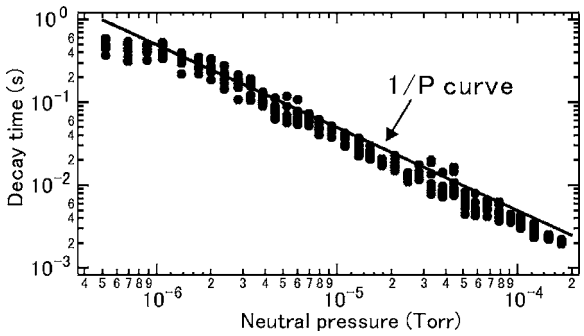

FIG. 6. Confinement time as a function of added neutral gas (hydrogen) pressure. $I_{TF}=10.5$ kAT, $V_{IC}=-300$ V.

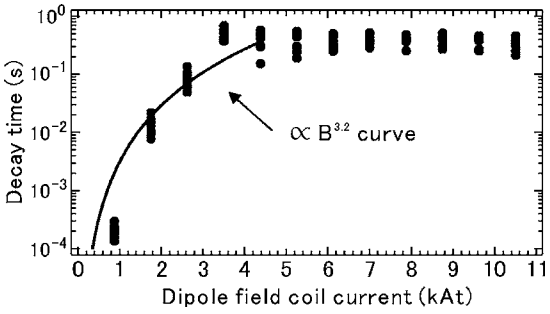

FIG. 7. Confinement time as a function of the dipole magnetic field strength.

$$\tau_D \sim a/v_r = \frac{eaB^3}{m_e n_n \sigma E^2} \propto P^{-1}B^3,$$

where a is the minor radius of the electron plasma. Substituting the experimental parameters of $B \sim 0.005$ T, $P = 10^{-6}$ Torr, $E = 3 \times 10^2$ V m^{-1}, $\sigma \sim 10^{-19}$ m^2, and $a = 0.1$ m, the typical confinement time τ_D is in the order of 1 s, and is comparable to the observed confinement time. For the pressure range of 10^{-6} to 10^{-4} Torr, τ is scaled as $\propto P^{-1}$, as shown in Fig. 6, indicating that the effects of residual neutral gas set the confinement time. When P is below $\sim 10^{-6}$ Torr, τ deviates from the P^{-1} line and saturates near 0.5 s. The confinement time at the base pressure of 4×10^{-7} Torr in the variation of the dipole field coil current is shown in Fig. 7. Before entering the saturation region (when I_{IC} is below ~ 5 kAT), the observed τ is approximately proportional to B^3 and it also agrees with the parameter dependence of the calculated τ_D, but τ has an upper limit in spite of the increase of the magnetic field strength above $I_{IC} \sim 5$ kAT. As indicated in the change of the electron charge in Fig. 8, the amount of the trapped charge as well as τ saturate above $I_{IC} \sim 5$ kAT, although the obtained electron density ($\sim 10^{12}$ m^{-3}) is far below the Brillouin density limit ($\sim 10^{14}$ m^{-3}), suggesting the existence of some anomalous loss of the electrons.

In the initial large fluctuation phase just after the stop of the electron injection, the charge on the wall decreased from ~ 200 pC to 32 pC, and only a small fraction of electrons showed good confinement properties. In comparison with the trapped charge during the electron injection calculated from the Poisson's equation, the stably confined electron charge is estimated to be $\sim 5 \times 10^{-8}$ C when $I_{IC} = 10.5$ kAT, $P = 4 \times 10^{-7}$ Torr, and $V_{IC} = -300$ V.

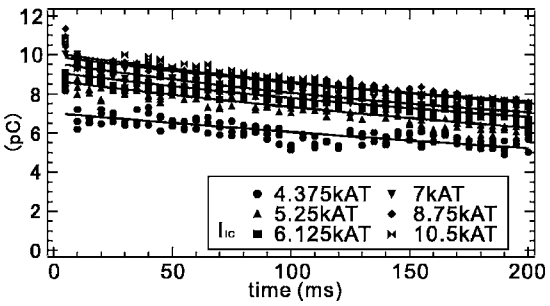

FIG. 8. Decay of trapped charge on the wall in the variation of the dipole field coil current.

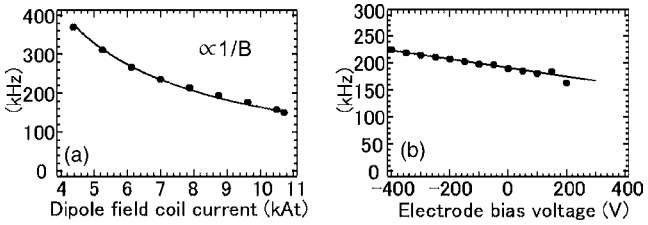

FIG. 9. Fundamental frequencies of wall probe signal during the electron injection, in the variation of (a) dipole magnetic field strength and (b) bias voltage of the IC electrode, V_{IC}.

As described in the previous section, the high density region of the electron plasma is located relatively far from the coolant structures of the internal conductor. Such a distribution of the plasma can be interpreted as the results of the mirror trap of some of the electrons in the weaker magnetic field region. The beam component of electrons in the "passing orbit" can be readily lost due to the collisions with obstacles in the device, but the mirror-trapped bulk component of electrons may show the observed longer confinement time. There are also electrostatically trapped electrons because of the negatively biased electrode, because some of the dipole magnetic field lines intersect the internal conductor. These electrons can undergo reflection in the poloidal direction and toroidal $\mathbf{E} \times \mathbf{B}$ drift motions without hitting the coolant and support structures.

B. Electrostatic fluctuations

The frequencies of the oscillation during the electron injection phase are shown in Fig. 9 as functions of the magnetic field strength and V_{IC}. The frequency is inversely proportional to the magnetic field strength and shows an approximately linear dependence on the external electric fields. When the IC electrode is more positively biased than $\sim +200$ V, a clear peak of frequency was not observed in the power spectrum, suggesting that the electrons are not confined as plasma.

Assuming the axisymmetry of the plasma and the device configuration, the energy source for the diocotron mode in the dipole field is the shear in the toroidal flow velocity v_t, and the wave is expected to propagate in the cross-field toroidal direction.[21] As well as the characteristics of the fluctuation frequencies, the direction of the wave propagation also agrees with the properties of diocotron oscillation mode. The waveforms of two wall probes in the pure poloidal (dipole) field and dipole and toroidal fields configurations are shown in Fig. 10. The walls are located at $Z = \pm 20$ cm in the same poloidal cross section of the device. In a pure poloidal magnetic field, the oscillations have no phase difference in the poloidal direction and the wave propagates in the toroidal direction. The addition of a toroidal field results in a phase difference between the two wall probe signals, as indicated in the lower part of Fig. 10.

When observed at $Z = \pm l/2$ in the same poloidal cross section, the phase shift ϕ between two walls located in a wave propagating in the cross fields direction is given by

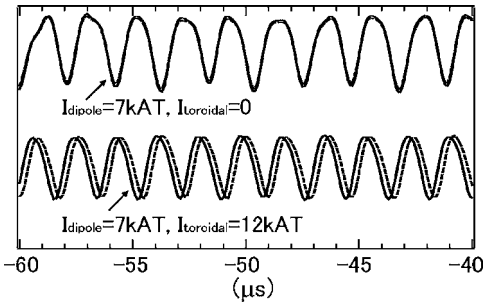

FIG. 10. Waveforms of the wall probes located at $Z=+20$ cm (solid lines) and $Z=-20$ cm (dotted lines) in the same poloidal cross section of the device. Fluctuations during the electron injection in a pure dipole field (upper lines), and dipole and toroidal fields (lower lines).

$$\phi = 2\pi l \sin\theta/\lambda,$$

where λ is the wavelength and θ is the pitch angle between the toroidal and poloidal fields. Here, the plasma shape is supposed to be azimuthally symmetric and the plasma has only a radial electric field. Figure 11 shows the observed phase difference between two walls at $Z=\pm 20$ cm in the variation of added toroidal field strength, while the strength of the poloidal (dipole) field was kept constant. The solid line shows the calculated ϕ, obtained by substituting the field strength at $R=40$ cm and taking the toroidal circumference of the device with a major radius of $R=40$ cm as the typical wavelength λ of $n=1$ mode. The observed phase shift of two wall probes shows similar dependence on the toroidal field strength with the calculated ϕ, the phase difference of the diocotron mode in the poloidal and toroidal magnetic fields. The disagreement in the stronger toroidal field region possibly occurred because λ was simply assumed to be constant in the calculation of ϕ, and the effects of the increase of λ due to the spiral orbit are neglected.

The power spectrum of the fluctuation during the electron injection is shown in Fig. 12. When the toroidal field is added to the dipole magnetic field, the power of the fundamental mode decreases and the second harmonic component becomes dominant. Although the present measurement was done only in one poloidal cross section of the device and the mode patterns of the oscillation were not specified, the observation may suggest that the $n=2$ mode is dominant in the pure dipole field and is damped under the sheared magnetic field. As described in Fig. 12(c), when $I_{TF}=30$ kAT and $I_{IC}=7$ kAT, the amplitude of the total fluctuation decreases by a factor of 10, compared with when in the pure dipole field configuration, while the generated space potential is kept approximately constant (ϕ_H at $R=46$ cm is between 230 V and 290 V, for the variation of I_{IC} from 7 kAT to 30 kAT), and stabilization of the diocotron instability by magnetic shear[22] is experimentally demonstrated.

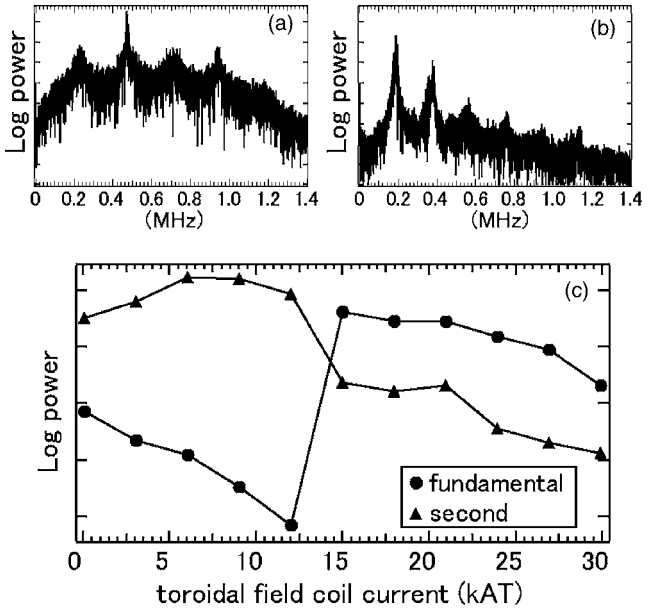

FIG. 12. Power spectrum of wall signals when (a) $I_{IC}=7$ kAT and $I_{TF}=0$ and (b) $I_{IC}=7$ kAT and $I_{TF}=30$ kAT. (c) Intensity ratio of the fundamental and second harmonics mode in the variation of I_{TF}. $I_{IC}=7$ kAT.

Although the addition of a toroidal magnetic field is effective for the realization of quiet plasma during the electron injection, it induces the onset of the rapid growth of instability after the electron injection is stopped. As shown in the lifetime of the electron plasma in Fig. 13, the plasma tends to disrupt in the long confinement phase as the stronger toroidal field is added. Similarly, when Langmuir probes or other structures are inserted into the confinement region, reduction of the lifetime is also observed even in the pure dipole field configuration. One of the possible interpretations is that when electrons hit the surfaces of the obstacles, accumulated neutral gas molecules are released and ionized, which causes ion resonance instability.[23,24] In the dipole and toroidal fields configuration, the $\mathbf{E}\times\mathbf{B}$ drift motions of electrons take spiral orbits around the internal conductor, and the trajectories may intersect the coolant and feeder structures of the internal con-

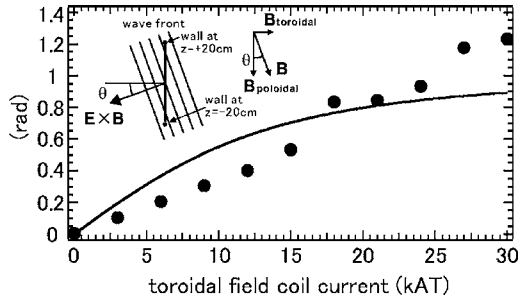

FIG. 11. Phase difference of wall signals at $Z=\pm 20$ cm (circles) and calculated phase difference ϕ (solid line).

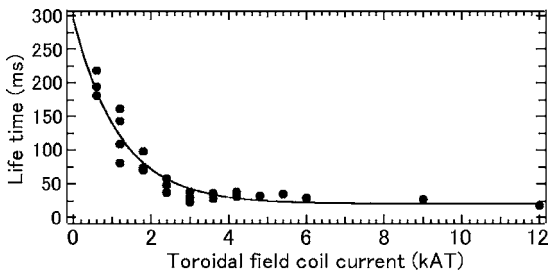

FIG. 13. Lifetime of electron plasma in the variation of I_{TF}. $I_{IC}=7$ kAT is kept constant.

ductor, which lead to the collisions of electrons with obstacles. Although the trajectories of some of the electrons in the "trapped" orbits do not intersect the obstacles, electrons in the "passing" orbits can be lost due to the collisions with the obstacles. Because the strength of the toroidal field is comparable to the dipole field strength in Proto-RT, the toroidal component of the flow velocity caused by the addition of a toroidal field is much larger than that induced by the $\mathbf{E}\times\mathbf{B}$ drift in the pure dipole field. The effects of such a large pitch angle spiral motion lead to the reduction of the mean path length of electrons before hitting the obstacles. These adverse effects of the internal coil structures might be solved in a stellarator[9] or superconducting levitated ring device[7] in future experiments.

IV. CONCLUSION

In the Proto-RT device, toroidal pure electron plasma has been confined in the magnetic surface configuration for as long as the classical diffusion time. When we adjusted the equipotential contours to the magnetic surfaces, the initial fluctuation damps and the trapped electron plasma enters a quiescent phase. In the present device parameters of $B \sim 10^{-2}$ T and $P=4\times10^{-7}$ Torr, electrons with a peak density of an order of 10^{12} m^{-3} and total charge of $\sim5\times10^{-8}$ C were confined for $\tau\sim0.5$ s. Magnetically or electrostatically mirror trapped electrons were located in the weak magnetic field region, and their orbits were not seriously disturbed by the support structures for the internal conductor. When τ is below ~0.1 s, it was scaled as $\tau\propto P^{-1}B^3$ for the pressure range between 10^{-6} and 10^{-4} Torr, indicating that the collisions with remaining neutral gas limit the confinement of electrons. In the lower pressure region of below $\sim10^{-6}$ Torr, τ saturates above ~0.1 s, suggesting the anomalous loss of electrons. Although the stabilizing effects of magnetic shear are observed, the addition of the toroidal field shortens the stable confinement time, possibly because of the obstacles of the support structure for the internal conductor.

ACKNOWLEDGMENTS

The authors would like to thank Mr. J. Morikawa and Professor H. Himura for useful discussions and for advice on the experiment.

This work was funded by a Grant-in-Aid for Scientific Research No. 14102033 from MEXT of Japan. The work of H.S. was supported in part by JSPS Research Fellowship for Young Scientist.

[1] J. D. Daugherty and R. H. Levy, Phys. Fluids **10**, 155 (1967).
[2] J. D. Daugherty, J. E. Eninger, and G. S. Janes, Phys. Fluids **12**, 2677 (1969).
[3] A. Mohri, M. Masuzaki, T. Tsuzuki, and K. Ikuta, Phys. Rev. Lett. **34**, 574 (1975).
[4] W. Clark, P. Korn, A. Mondelli, and N. Rostoker, Phys. Rev. Lett. **37**, 592 (1976).
[5] P. Zaveri, P. I. John, K. Avinash, and P. K. Kaw, Phys. Rev. Lett. **68**, 3295 (1992).
[6] S. S. Khirwadkar, P. I. John, K. Avinash, A. K. Agarwal, and P. K. Kaw, Phys. Rev. Lett. **71**, 4334 (1993).
[7] Z. Yoshida, Y. Ogawa, J. Morikawa *et al.*, in *Nonneutral Plasma Physics III*, AIP Conf. Proc. No. 498 (AIP, New York, 1999).
[8] H. Saitoh, Z. Yoshida, C. Nakashima, H. Himura, J. Morikawa, and M. Fukao, Phys. Rev. Lett. **92**, 255005 (2004).
[9] T. S. Pedersen and A. H. Boozer, Phys. Rev. Lett. **88**, 205002 (2002).
[10] M. R. Stoneking, P. W. Fontana, R. L. Sampson, and D. J. Thuecks, Phys. Plasmas **9**, 766 (2002).
[11] M. R. Stoneking, M. A. Growdon, M. L. Milne, and R. T. Peterson, Phys. Rev. Lett. **92**, 095003 (2004).
[12] H. Himura, H. Wakabayashi, M. Fukao, and Z. Yoshida, Phys. Plasmas **11**, 492 (2004).
[13] D. H. E. Dubin and T. M. O'Neil, Rev. Mod. Phys. **71**, 87 (1999).
[14] A. Mohri, H. Higaki, H. Tanaka, Y. Yamazawa, M. Aoyagi, T. Yuyama, and T. Michishita, Jpn. J. Appl. Phys., Part 1 **37**, 664 (1998).
[15] F. Anderegg, E. M. Hollmann, and C. F. Driscoll, Phys. Rev. Lett. **81**, 4875 (1998).
[16] A. H. Boozer, Phys. Plasmas **11**, 4709 (2004).
[17] D. L. Eggleston, Phys. Plasmas **4**, 1196 (1997).
[18] C. Nakashima, Z. Yoshida, H. Himura, M. Fukao, J. Morikawa, and H. Saitoh, Phys. Rev. E **65**, 036409 (2002).
[19] C. Nakashima, Ph.D. thesis, Department of Quantum Engineering and System Sciences, University of Tokyo (2002).
[20] H. Saitoh, Z. Yoshida, and C. Nakashima, Rev. Sci. Instrum. **73**, 87 (2002).
[21] S. Pradhan and K. Avinash, Phys. Fluids B **5**, 2334 (1993).
[22] S. Kondoh, T. Tatsuno, and Z. Yoshida, Phys. Plasmas **8**, 2635 (2001).
[23] R. H. Levy, J. D. Daugherty, and O. Buneman, Phys. Fluids **12**, 2616 (1969).
[24] A. J. Peurrung, J. Notte, and J. Fajans, Phys. Rev. Lett. **70**, 295 (1993).